PERIÓDICO TCHÊ QUÍMICA
ARTIGO ORIGINAL

AVALIAÇÃO DA FORÇA DE UM PACOTE COMPOSTO COM DEFEITOS INTERNOS DE ACORDO COM VÁRIOS CRITÉRIOS DE FALHAS SOB A INFLUÊNCIA DE CARGA INDEPENDENTE

ASSESSMENT OF THE STRENGTH OF A COMPOSITE PACKAGE WITH INTERNAL DEFECTS ACCORDING TO VARIOUS FAILURES CRITERIA UNDER THE INFLUENCE OF UNSTEADY LOAD

MEDVEDSKIY, Aleksandr L.[1*]; MARTIROSOV, Mikhail I.[2]; KHOMCHENKO, Anton V.[3]; DEDOVA, Darina V.[4];

[1] Central Aerohydrodynamic Institute, 1 Zhukovsky Str., zip code 140180, Zhukovsky – Russian Federation

[2,4] Moscow Aviation Institute (National Research University); Department of Resistance of Materials, Dynamics, and Strength of Machines; 4 Volokolamskoe Highway; zip code 125993; Moscow – Russian Federation

[3] JSC "Irkut Corporation", Design Bureau of the Engineering Center, 68 Leningradsky Ave., zip code 125315, Moscow – Russian Federation

** Correspondence author*
e-mail: mdv66@mail.ru

Received 22 March 2020; received in revised form 29 June 2020; accepted 07 July 2020

RESUMO

Uma das tarefas prioritárias para a indústria aeronáutica moderna é alevar a eficiência econômica das aeronaves. No contexto da solução deste problema, ao criar novas aeronaves, os materiais compostos de polímeros (PCM) são cada vez mais utilizados. É dada especial atenção aos elementos estruturais, cujos danos podem levar a diminuição da resistência geral da estrutura. Portanto, uma tarefa essencial no projeto, manutenção e operação do teste é estudar o efeito de defeitos entre camadas na resistência e no comportamento das estruturas de PCM sob a influência de cargas instáveis. Este trabalho foi dedicado a análise numérica do comportamento de uma placa feita de material compósito de polímero (PCM) sob carga instável, considerando defeitos intercamadas de forma elíptica, bem como uma avaliação da resistência de uma embalagem compósita de acordo com várias fraturas critério. O problema foi resolvido pelo método dos elementos finitos usando o pacote de *software* LS-DYNA. Em seguida, utilizando o método de modelagem matemática, analisou-se a separação entre camadas de uma forma elíptica, que permitiu avaliar a resistência da placa e da fibra de acordo com os critérios de Hashin, Puck, Chang-Chang e LaRC03 e comparar os resultados. Verificou-se no estudo que os índices de falha e os fatores de segurança, obtidos através de vários critérios (Hashin e Chang-Chang), têm a mesma distribuição, desde a dependência do modo de fratura implementado (compressão da fibra na direção longitudinal) foi idêntico. Os materiais de análise podem ser levados em consideração ao desenvolver requisitos técnicos e montar estruturas de aeronaves.

Palavras-chave: *placa composta, critérios de falha em compósitos, defeito interlaminar, método dos elementos finitos (MEF), material compósito polimerico*.

ABSTRACT

One of the priority tasks of the modern aviation industry is to increase the economic efficiency of aircrafts. In the context of solving this problem, when creating new aircrafts, polymer composite materials (PCM) are increasingly used. Particular attention is paid to structural elements, damage to which can lead to a decrease in the strength of an airframe as a whole. Therefore, an essential task in the design, maintenance, and operation of the test is to study the effect of interlayer defects on the strength and behavior of PCM structures under the influence of unsteady loads. This work is devoted to a numerical analysis of the behavior of a plate made of a polymer composite material (PCM) under unsteady load considering interlayer defects of an elliptical shape, as well as an assessment of the strength of a composite package according to various fracture criteria. The problem is solved by the finite element method using the LS-DYNA software package. Then, using the method of mathematical modeling, the interlayer separation of an elliptical shape was analyzed, which allowed to evaluate the strength of the plate and fiber according to the criteria of Hashin, Puck, Chang-Chang, and LaRC03 and

DOI: 10.52571/PTQ.v17.n35.2020.100_MEDVEDSKIY_pgs_1218_1230.pdf

compare the results. It was found in the study, that the failure indices and safety factors, which were obtained using various criteria (Hashin and Chang-Chang), have the same distribution, since the dependence of the implemented fracture mode (fiber compression in the longitudinal direction) is identical. Analysis materials can be taken into account when developing technical requirements and assembling aircraft structures.

Keywords: *composite plate, composites failure criteria, interlaminar defect, finite element method (FEM), polymer composite material.*

1. INTRODUCTION

Appropriate calculations and full-scale tests must support the structural strength of the PCM in the aviation industry. Particular attention is given to the structural elements, damage which can lead to a decrease in airframe structural strength in general. The result of such damages may be interlayer defects such as bundles (Nia *et al.*, 2020; Shen *et al.*, 2020; Tian *et al.*, 2020).

Interlaminar defects can occur at various stages, both at the production stage and during operation. Among the main reasons that can cause defects, we can distinguish the following: a collision with a bird, hit stones on takeoff, non-localized dispersion of the engine rotor, hit fragments pneumatics, hit hail, collision when towing or steering with aerodrome infrastructure facilities, falling tool or replacement part (Koh and Madsen, 2018; Valverde *et al.*, 2020).

The resulting defects at selected non-destructive testing methods (including ultrasonic flaw detection, x-ray, current-vortex, optical holography, acoustic monitoring) are divided into undetectable, detectable with any form of control, reliably detected within several flights by technical personnel and evident to the crew (Miranda Guedes, 2019). The presence of defects in the structure of the PCM elements can lead to cracking of the binder, fiber destruction, and loss of strength of the composite packet (CP) (Kulkarni *et al.*, 2020). It follows that an essential task for the design, maintenance, and operation of the test is to study the influence of interlaminar defects on the strength and behavior of PCM constructions under the influence of unsteady loads (Ershova *et al.*, 2018; Medvedskiy *et al.*, 2019; Medvedsky *et al.*, 2019a; Medvedsky *et al.*, 2019b; Medvedsky *et al.*, 2019c; Medvedsky *et al.*, 2019d; Medvedsky *et al.*, 2019e). This paper shows the results of numerical simulation of the behavior of a rectangular plate made of a layered composite in the presence of interlayer defects of the bundle type. The impact of a spherical blast wave formed after the detonation of a point source is considered as an external non-stationary load. In solving the problem, we used the finite element method (FEM) implemented in the LS-DYNA software package using an explicit time integration scheme for the complete system of FEM equations (Bento Rebelo and Cismaşiu, 2017; Trajkovski, 2017a; Trajkovski, 2017b; Erdik and Uçar, 2018; Teng, 2018; Bisyk *et al.*, 2019). The distribution of pressure on the outer surface of the plate, deflections in the zone of defects at different times were obtained, as well as the analysis of the operating stresses and deformations in the layers of the plate, and based on this analysis, the maximum failure indices and minimum safety factors in the most loaded layer were determined according to various failure criteria for composite materials (Chen *et al.*, 2020; Rena *et al.*, 2020). A comparison of the considered failure criteria for a point with a minimum safety factor is performed, and a graph of changes in the failure indices at various points in time is presented. A quantitative assessment of the degree of reduction of the minimum safety factor in the presence of multiple elliptic defects between the layers of the plate is made. The proposed method allows us to take into account the presence of interlayer defects of various shapes, sizes and layouts between the layers of the package under the action of a wide range of non-stationary loads: the action of pressure fields distributed according to different laws, the impact of a striker with different speed and energy, the action of acoustic and explosive waves generated by different sources, the impact of temperature fields.

The consideration of interlayer effects with allowance for temperature factors was considered. This work is devoted to the numerical analysis of the behavior of the plate of a polymer composite material (PCM) under unsteady load considering interlayer defects elliptical shape, as well as evaluating the strength of the compositey package according to various failure criteria.

2. MATERIALS AND METHODS

The object of this research is a rectangular plate made of PCM length a = 500 mm and a width b = 200 mm (Figure 1). The plate is made of carbon fiber using autoclave technology based on

prepreg HexPly M21/34%/UD194/IMA (IMA carbon tape-based high-strength fiber HexTow IMA-12K and modified epoxy binder M21) manufactured by Hexcel Composites (USA). The thickness of the mono-layer is assumed to be equal to h = 0.184 mm. Laying plate has the following scheme: [+45°/-45°/90°/0°/+45°/-45°/-45°/+45°/0°/90°/-45°/+45°] (total of 12 mono-layer, 2.208 mm total thickness of the package).

The problem is solved by the finite element method (FEM) in the software package LS-DYNA. Each mono-layer modeled a separate set of finite elements with the wording "16: Fully integrated shell element" and property "COMPOSITE". It is assumed that between all layers, there are defects in the form of interlaminar delamination of elliptical shape with axes of 60 and 40 mm. The layers, except for the defect zones, are connected by a glue contact "Automatic One-Way Surface to Surface Tiebreak". The "Automatic Surface to Surface" contact is taken into account between defects.

As an external unsteady load, an explosive impact with a spherical blast wave is used, which is modeled using the "Load Blast Enhanced" function based on the Kingery-Bulmash model (Le Blanc *et al.*, 2005; Tabatabaei and Volz, 2012; Schwer *et al.*, 2015). The epicenter of the explosion is located above the defects at a distance of 300 mm, and the detonation energy is E = 33.47 kJ. As boundary conditions, the hinge support along the long edges of the plate is used. To assess the strength of a PCM plate, the following failure criteria are used to evaluate the strength of the matrix and the fiber separately: Hashin (1980), Puck (Puck and Schurmann, 1998), Chang and Chang (1987), LaRC03 (Sebaey *et al.*, 2011; Muizemnek and Kartashova, 2017). Appropriate depending is shown below1. Criteria Hashin. Fiber strength for plane stress state is determined by the following Equations (1)-(2).

The strength of the matrix (Equations 3-4), where f_f – fiber failure index, f_m – matrix failure Index, σ_1 – normal stress acting in the longitudinal direction, σ_2 – normal stress acting in the lateral direction, τ_{12} – shear stress acting in the plane, X_T – tensile strength in the longitudinal direction at a stretching, X_C – tensile strength in the longitudinal direction at a compression, Y_T – tensile strength in the transverse direction at a stretching, Y_C – tensile strength in the transverse direction under compression, S_{12} – shear strength in the plane. Failure occurs when one of the Equations (1)-(4) becomes equal to unity. Hashin failure index can be written as (Equation 5).

2. Criterion Puck. Fiber strength is determined by the following Equations (6)-(7). The strength of the matrix (Equations 8-13), where (Equations 12-13), f_{mA}, f_{mB}, f_{mC} – form of failure of the matrix. For carbon fiber reinforced plastics $p_{12}^{(+)} = 0.3$, $p_{12}^{(-)} = 0.35$, $p_{22}^{(+)} = p_{22}^{(-)} = 0.25\text{-}0.3$.

3. Criterion Chang-Chang. Strength fibers for plane stress state are determined by the following Equations (14)-(18). Fiber strength was determined using Equations (14), (15). The strength of the matrix was determined using Equations (16)-(18), where β – taken equal to 0.1.

4. Criterion LaRC03 (Chen *et al.*, 2018) Equations (19)-(25), where ε_1 – the deformation is exerted in the longitudinal direction by stretching; ε_1^T – limiting deformation in the longitudinal direction at a stretching, σ_{22}^m, τ_{12}^m – stresses in areas of misalignment, η^L – longitudinal friction coefficient, Y_{is}^T, S_{is}^L – the limits of local strength, g, (G_{IC}/ G_{IIC}) – fracture stiffness coefficient, τ_{eff}^T, τ_{eff}^T – effective shear stress in compression of the matrix calculated based on the Mohr-Coulomb criterion, which binds effective shear stress in the disk Mora failure plane (Equation 26), where $\alpha_0 = 53$ – fracture angle.

Material mono-layer has the following mechanical characteristics: X_T = 2830 MPa, X_C = 1500 MPa, Y_T = 54 MPa, Y_C = 271 MPa, S_{12} = 96 MPa, E_1 = 178 GPa, E_2 = 8.6 GPa, G = 3.0GPa, μ_{12} = 0.32, ρ = 1580 kg / m^3. Here μ_{12} – Poisson ratio, which characterizes the lateral contraction in the longitudinal direction, G – shear modulus in the plane of the sheet, ρ – density, E_1 – elasticity module in the longitudinal direction, E_2 – modulus of elasticity in the transverse direction. Characteristics mono-layer received PKM manufacturer experimentally according to European standards EN samples for RTD mode (Room Temperature Dry): normal temperature +23 °*C* and the humidity – in the delivery state (Antufev *et al.*, 2019; Kuznetsova and Rabinskiy, 2019).

3. RESULTS AND DISCUSSION:

Figure 2 shows the variation of the external pressure on the surface of the plate in the center location of the defects as a result of the detonation wave. Figures 3-4 shows the stress distribution in the longitudinal direction and shear stresses in the layer No. 10 (90°) at a time 0.59 ms in cases of presence and absence of defects between the layers. Figures 5-7 show the distribution of safety factors in layer 10 (90°) at the time of 0.59 m s for

cases of presence and absence of defects between layers according to various failures criteria. Figure 8 shows the distribution of pressure from the blast wave action on the surface of the plate at a time 0.59 ms. Figures 9-10 show displacement along the major axis of the defect in the layer No. 10 at different time points for the plate in the presence and absence of defects, respectively. Figures 9-10 show that for layer 10, the maximum displacement values differ slightly, but the behavior is different. This is due to the presence of defects between layers. Figure 11 shows the variation of failure index at the point with a minimum safety factor for any failure criteria.

Thus, from Figures 3-7, it is seen that in case of a defect, the maximum-acting guides longitudinal stresses above about 1.68 times compared with the case of absence of defects. Analysis of the distribution failure indexes and safety factors obtained by different failure criteria showed that criteria Hashin and Chang-Chang have the same distribution because the dependence of the realized form of destruction (fiber compression in the longitudinal direction) is the same. The minimum safety factor was calculated from LaRC03 criterion ("η = 0.87") decrease in strength of the structure in case of the presence of defects LaRC03 criterion is 2.46 times.

4. CONCLUSIONS:

Thus, the behavior of a laminate plate made of a polymer composite material under non-stationary load taking into account interlayer defects of an elliptical shape was studied, as well as the strength of the composite package according to various fracture criteria was assessed. The pressure distribution on the outer surface of the plate under the influence of an air blast wave is determined. The deflections of the plate along the defect are also determined in the presence and absence of interlayer defects. The analysis of these dependencies shows a difference in the behavior of the plate in the defect zone. The dependences of the failure indices on the considered failure criteria at various moments in time are determined. An analysis of distribution failure indices and safety factors obtained using different failure criteria showed that the Hashin and Chang-Chang criteria have the same distribution since the dependence of the realized fracture shape (longitudinal compression of the fiber) is the same. For the design under consideration, the presence of a defect reduces the strength by 2.46 times, the minimum safety factor is implemented using the LaRC03 criterion and is 0.87. The results of the analysis can be taken into account when developing technical requirements and assembling the structures of an aircraft including when exposed to temperature fields.

5. ACKNOWLEDGMENTS:

The work was conducted at the Moscow Aviation Institute with financial support from the Russian Foundation for Basic Research, project No. 18-08-01153.

6. REFERENCES:

1. Antufev, B. A., Kuznetsova, E. L., Rabinskiy, L. N., and Tushavina, O. V. (2019). Complex stressed deformed state of a cylindrical shell with a dynamically destructive internal elastic base under the action of temperature fields of various physical nature. *Asia Life Sciences*, *2*, 775-782.
2. Bento Rebelo, H., and Cismaşiu, C. (2017). *A comparison between three air blast simulation techniques in LS-DYNA.* Paper presented at the 11th European LS-DYNA Conference 2017, Salzburg, Austria.
3. Bisyk, S., Davydovskyi, L. S., Hutov, I., Slyvins'kyi, O. A., Aristarkhov, O. M., and Lilov, I. (2019). Comparison of numerical methods for modeling the effect of explosion on protective structures. *International Scientific Journal "Trans Motauto World"*, *4*(1), 20-23.
4. Chang, F. K., and Chang, K. Y. (1987). A progressive damage model for laminated composites containing stress concentration. *Journal of Composite Materials*, *21*, 834-855.
5. Chen, M., Zhang, D., and Gong, J. (2018). Predictions of transverse thermal conductivities for plain weave ceramic matrix composites under in-plane loading. *Composite Structures*, 202, 59-767.
6. Chen, Y., Zhao, Y., He, C., Ai, S., Lei, H., Tang, L., and Fang, D. (2020). Yield and failure theory for unidirectional polymer-matrix composites. *Composites Part B: Engineering*, *164*, 612-619.
7. Erdik, A., and Uçar, V. (2018). On evaluation and comparison of blast loading methods used in numerical simulations. *Sakarya University Journal of Science*, *22*(5), 1385-1391.
8. Ershova, A. Y., Kuznersova, E. L., Martirosov,

M. I., and Rabinsky, L. N. (2018). Experimental determination of characteristics of crack-resistance of disperse-strangthened composites based on non-saturated polyesters. *Journal of Mechanical Engineering Research and Developments*, *41*(3), 33-36.

9. Hashin, Z. (1980). Failure Criteria for unidirectional fiber composites. *Journal of Applied Mechanics*, *47*, 329-334.
10. Koh, R., and Madsen, Bo. (2018). Strength failure criteria analysis for a flax fibre reinforced composite. *Mechanics of Materials*, *124*, 26-32.
11. Kulkarni, P., Mali, K. D., and Singh, S. (2020). An overview of the formation of fibre waviness and its effect on the mechanical performance of fibre reinforced polymer composites. *Composites Part A: Applied Science and Manufacturing*, *137*, Article number 106013.
12. Kuznetsova, E. L. and Rabinskiy, L. N. (2019). Heat transfer in nonlinear anisotropic growing bodies based on analytical solution. *Asia Life Sciences*, *2*, 837-846.
13. Le Blanc, G., Adoum, M., and Lapoujade, V. (2005). External blast load on structures – Empirical approach. Retrieved from https://www.dynalook.com/conferences/european-conf-2005/Leblanc.pdf.
14. Medvedskiy, A. L., Rabinskiy, L. N., Martirosov, M. I., Ershova, A. Yu., and Khomchenko, A. V. (2019). The study of changes in strength of polymer composite panels with interlayer defects under the action of unsteady load. *The Asian International Journal of Life Sciences*, *21*(1), 565 576.
15. Medvedsky, A. L., Martirosov, M. I., and Khomchenko, A. V. (2019a). Behavior of the shallow composite panel with initial defects at strike influence. *Izvestiya TulGU. Technical Science*, *12*, 159-163.
16. Medvedsky, A. L., Martirosov, M. I., and Khomchenko, A. V. (2019b). Dynamic of reinforced composite panel with mono-layer combined stacking with inner damages at non-stationary impacts. *Bulletin of Bryansk State Technical University*, *7*, 35-41.
17. Medvedsky, A. L., Martirosov, M. I., and Khomchenko, A. V. (2019c). Numerical analysis of layered composite panel behavior with interlaminar defects subject to dynamic loads. *Structural Mechanics of Engineering Construction and Buildings*, *15*(2), 127-134.
18. Medvedsky, A. L., Martirosov, M. I., and Khomchenko, A. V. (2019d). Numerical research of failure of the plane panel made polymer composite material with internal defects under action of non-stationary load. Aviation Industry. *Quarterly Scientific and Technical Magazine*, *1*, 52-56.
19. Medvedsky, A. L., Martirosov, M. I., and Khomchenko, A. V. (2019e). Numerical study of the behavior of a composite plate with multiple damages under dynamic loads. *Collection of Works of the XII All-Russian Congress on Fundamental Problems of Theoretical and Applied Mechanics*, *3*, 552-554.
20. Miranda Guedes, R. (2019). *Creep and fatigue in polymer matrix composites*. Sawston, England: Woodhead Publishing.
21. Muizemnek, A. Yu., and Kartashova, E. D. (2017). *Mechanics of deformation and destruction of polymer layered composite materials*. Penza, Russian Federation: Publishing House PSU.
22. Nia, X., Furtado, C., Fritz, N.K., Kopp, R., Camanho, P.P., and Wardle, B.L. (2020). Interlaminar to intralaminar mode I and II crack bifurcation due to aligned carbon nanotube reinforcement of aerospace-grade advanced composites. *Composites Science and Technology*, *190*, Article number 108014.
23. Puck, A., and Schurmann, H. (1998). Failure analysis of FRP laminates by means of physically based phenomenological models. *Composites Science and Technology*, *58*, 1045-1067.
24. Rena, Zh., Liu, L., Liu, Y., and Leng, J. (2020). Damage and failure in carbon fiber-reinforced epoxy filament-wound shape memory polymer composite tubes under compression loading. *Polymer Testing*, *85*, Article number 106387.
25. Schwer, L., Teng, H., and Souli, M. (2015). *LS-DYNA air blast techniques: Comparisons with experiments for close-in charges*. Paper presented at the 10th European LS-DYNA Conference, Würzburg, Germany.
26. Sebaey, T. A., Blanco, N., Lopes, C. S., and Costa, J. (2011). Numerical investigation to prevent crack jumping in Double Cantilever Beam test of multidirectional composite laminates. *Composites Science and Technology*, *71*, 1587-1592.
27. Shen, L., Liu, L., Zhou, Y., and Wu, Z. (2020). Thickness effect of carbon nanotube interleaves on free-edge delamination and

ultimate strength within a symmetric composite laminate. *Composites Part A: Applied Science and Manufacturing*, *132*, Article number 105828.

28. Tabatabaei, Z. S., and Volz, J. S. (2012). A comparison between three different blast methods in LS-DYNA: LBE, MM-ALE, coupling of LBE and MM-ALE. Retrieved from https://www.dynalook.com/conferences/12th-international-ls-dyna-conference/blast-impact20-d.pdf.
29. Teng, H. (2018). Scalability study of particle method with dynamic load balancing. Retrieved from https://www.semanticscholar.org/paper/Scalability-Study-of-Particle-Method-with-Dynamic-Teng/f78f0f20a5ce1d2620a8bd191207fbaa028244db.
30. Tian, K., Pan, Q., Deng, H., and Fu, Q. (2020). Shear induced formation and destruction behavior of conductive networks in nickel/polyurethane composites during strain sensing. *Composites Part A: Applied Science and Manufacturing*, *130,* Article number 105757.
31. Trajkovski, J. (2017a). *Comparison of MM-ALE and SPH methods for modelling blast wave reflections of flat and shaped surfaces.* Paper presented at the 11th European LS-DYNA Conference 2017, Salzburg, Austria.
32. Trajkovski, J. (2017b). MM-ALE Modelling Technique for Blast Response Analysis of Light Armoured Vehicles (LAV) According to AEP-55 Standard: Pros and Cons. *Key Engineering Materials*, *755*, 159-169.
33. Valverde, M. A., Kupfer, R., Wollmann, T., Kawashita, L. F., Gude, M., and Hallett, S. R. (2020). Influence of component design on features and properties in thermoplastic over-molded composites. *Composites Part A: Applied Science and Manufacturing*, *132*, Article number 105823.

$$f_f = \left(\frac{\sigma_1}{X_T}\right)^2 + \left(\frac{\tau_{12}}{S_{12}}\right)^2 = 1 \text{ at } \sigma_1 \geq 0 \quad \text{(Eq. 1)}$$

$$f_f = \left(\frac{\sigma_1}{X_C}\right)^2 = 1 \text{ at } \sigma_1 < 0 \quad \text{(Eq. 2)}$$

$$f_m = \left(\frac{\sigma_2}{Y_T}\right)^2 + \left(\frac{\tau_{12}}{S_{12}}\right)^2 = 1 \text{ at } \sigma_2 \geq 0 \quad \text{(Eq. 3)}$$

$$f_m = \left(\frac{\sigma_2}{Y_T}\right)^2 + \left(\frac{\tau_{12}}{S_{12}}\right)^2 = 1 \text{ at } \sigma_2 < 0 \quad \text{(Eq. 4)}$$

$$f = max\ (f_m, f_f) \quad \text{(Eq. 5)}$$

$$f_f = \frac{|\sigma_1|}{X_T} \text{ at } \sigma_1 \geq 0 \quad \text{(Eq. 6)}$$

$$f_f = \frac{|\sigma_1|}{X_C} \text{ at } \sigma_1 \leq 0 \quad \text{(Eq. 7)}$$

$$f_{mA} = \frac{1}{S_{12}}\left[\sqrt{\left(\frac{S_{12}}{Y_T} - p_{12}^{(+)}\right)^2 \sigma_2^2 + \tau_{12}^2} + p_{12}^{(+)}\sigma_2\right] \text{ at } \sigma_2 \geq 0 \quad \text{(Eq. 8)}$$

$$f_{mB} = \frac{1}{S_{12}}\left[\sqrt{\tau_{12}^2 + (p_{12}^{(-)}\sigma_2)^2} + p_{12}^{(-)}\sigma_2\right], \text{ if } \sigma_2 < 0,\ 0 \leq \left|\frac{\sigma_2}{\tau_{12}}\right| \leq \frac{Y^A}{\tau_{12C}} \quad \text{(Eq. 9)}$$

$$f_{mC} = \left(\left(\frac{\tau_{12}}{2\left(1+p_{12}^{(-)}S_{12}\right)}\right)^2 + \left(\frac{\sigma_2}{Y_C}\right)^2\right)\frac{Y_C}{|\sigma_2|}, \text{ if } \sigma_2 < 0,\ 0 \leq \left|\frac{\tau_{12}}{\sigma_2}\right| \leq \frac{\tau_{12C}}{Y^A} \quad \text{(Eq. 10)}$$

$$f = max\ (f_{mA}, f_{mB}, f_{mC}, f_f) \quad \text{(Eq. 11)}$$

$$\tau_{12C} = S_{12}\sqrt{1+2p_{22}^{(-)}},\ p_{22}^{(-)} = p_{12}^{(-)}\frac{Y^A}{S_{12}} \quad \text{(Eq. 12)}$$

$$Y^A = \frac{S_{12}}{2p_{22}^{(-)}}\left[\sqrt{1+2p_{12}^{(-)}\frac{Y_C}{S_{12}}} - 1\right] \quad \text{(Eq. 13)}$$

$$f_f = \left(\frac{\sigma_1}{X_T}\right)^2 + \beta\left(\frac{\tau_{12}}{S_{12}}\right) = 1 \text{ at } \sigma_1 \geq 0 \quad \text{(Eq. 14)}$$

$$f_f = \left(\frac{\sigma_1}{X_C}\right)^2 = 1 \text{ at } \sigma_1 < 0 \quad \text{(Eq. 15)}$$

$$f_m = \left(\frac{\sigma_2}{Y_T}\right)^2 + \left(\frac{\tau_{12}}{S_{12}}\right)^2 = 1 \text{ at } \sigma_2 \geq 0 \quad \text{(Eq. 16)}$$

$$f_m = \left(\frac{\sigma_2}{2S_{12}}\right)^2 + \left[\left(\frac{\sigma_2}{2S_{12}}\right)^2 - 1\right]\frac{\sigma_2}{Y_C} + \left(\frac{\tau_{12}}{S_{12}}\right)^2 = 1 \text{ at } \sigma_2 < 0 \quad \text{(Eq. 17)}$$

$$f = max\ (f_m, f_f) \quad \text{(Eq. 18)}$$

$$f_f = \frac{\varepsilon_1}{\varepsilon_1^T} \text{ at } \sigma_1 \geq 0 \quad \text{(Eq. 19)}$$

$$f_f = \frac{\varepsilon_1}{\varepsilon_1^T} \text{ at } \sigma_1 \geq 0 \quad \text{(Eq. 20)}$$

$$f_f = \frac{|\tau_{12}^m| + \eta_L \sigma_{22}^m}{S_{is}^L} \text{ at } \sigma_1 < 0 \text{ and } \sigma_{22}^m < 0 \quad \text{(Eq. 21)}$$

$$f_f = g\left(\frac{\sigma_{22}^m}{Y_{is}^T}\right)^2 + \left(\frac{\tau_{12}^m}{S_{is}^T}\right)^2 + (1-g)\left(\frac{\sigma_{22}^m}{Y_{is}^T}\right) \text{ at } \sigma_1 < 0 \text{ and } \sigma_{22}^m \geq 0 \quad \text{(Eq. 22)}$$

$$f_m = g\left(\frac{\sigma_2}{Y_{is}^T}\right)^2 + \left(\frac{\tau_{12}}{S_{is}^T}\right)^2 + (1-g)\left(\frac{\sigma_2}{Y_{is}^T}\right) \text{ at } \sigma_2 \geq 0 \quad \text{(Eq. 23)}$$

$$f_m = g\left(\frac{\tau_{eff}^T}{S^T}\right)^2 + \left(\frac{\tau_{eff}^L}{S_{is}^L}\right)^2 \text{ at } \sigma_1 \geq -Y_C \text{ and } \sigma_2 < 0 \quad \text{(Eq. 24)}$$

$$f_m = g\left(\frac{\tau_{eff}^{mT}}{S^T}\right)^2 + \left(\frac{\tau_{eff}^{mL}}{S_{is}^L}\right)^2 \text{ at } \sigma_1 < -Y_C \text{ and } \sigma_2 < 0 \quad \text{(Eq. 25)}$$

$$S^T = Y_C \cos(\alpha_0)\left(\sin(\alpha_0) + \frac{\cos(\alpha_0)}{\tan(2\alpha_0)}\right) \quad \text{(Eq. 26)}$$

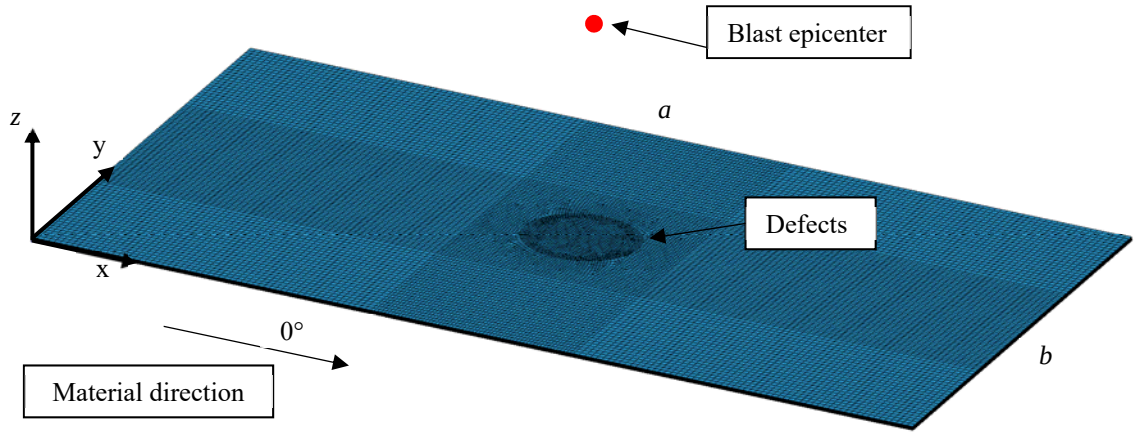

Figure 1. *Rectangular composite plate*

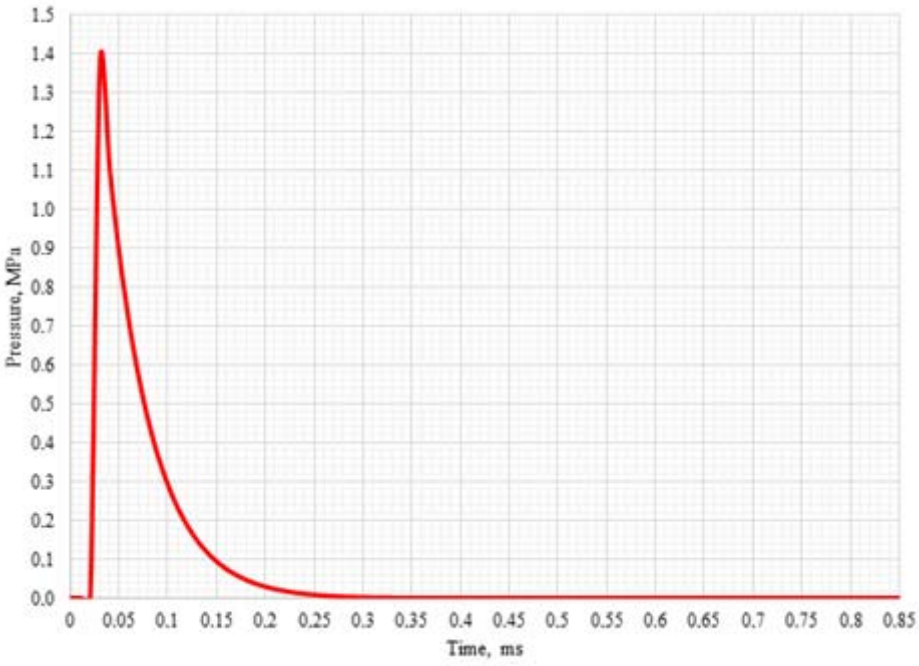

Figure 1. *Pressure change*

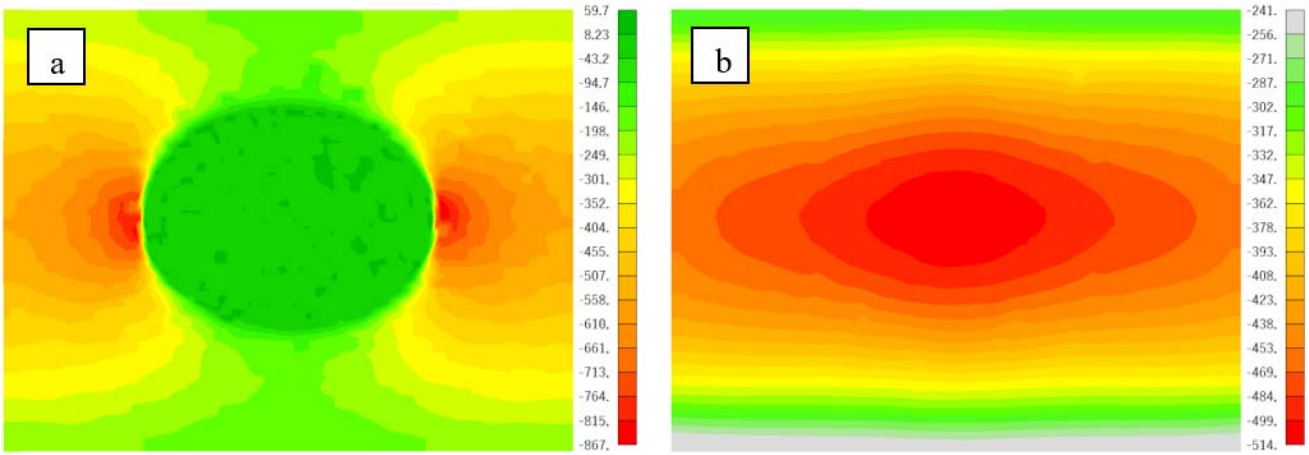

Figure 2. *Normal longitudinal stresses at 0.59 ms, MPa: a – with defects; b – without defects*

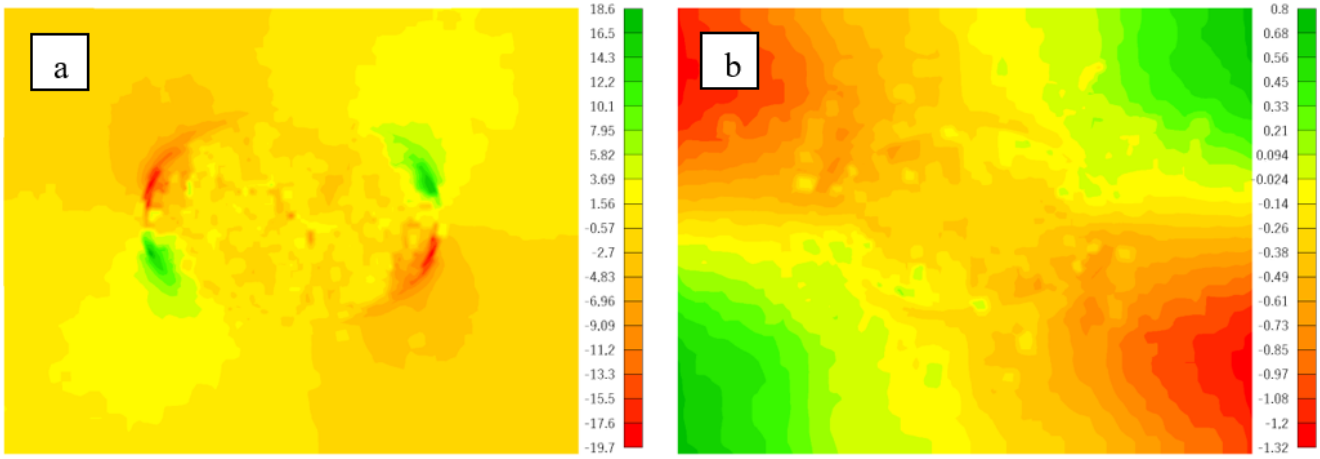

Figure 3. *Shear stresses at 0.59 ms, MPa: a – with defects; b – without defects*

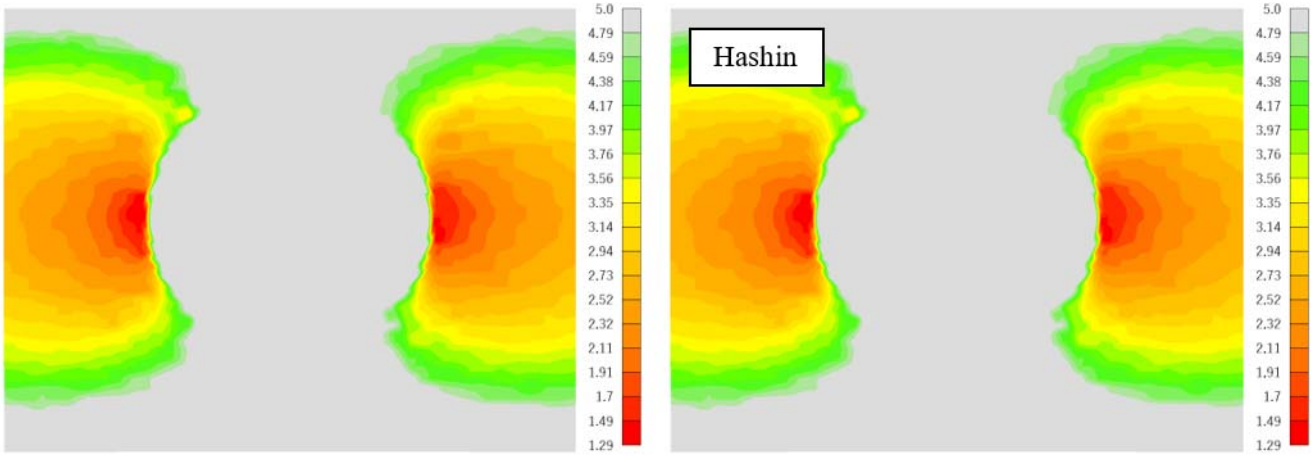

Figure 4. *Safety factors at 0.59 ms for the plate with defects*

Source: Hashin (1980), Chang and Chang (1987).

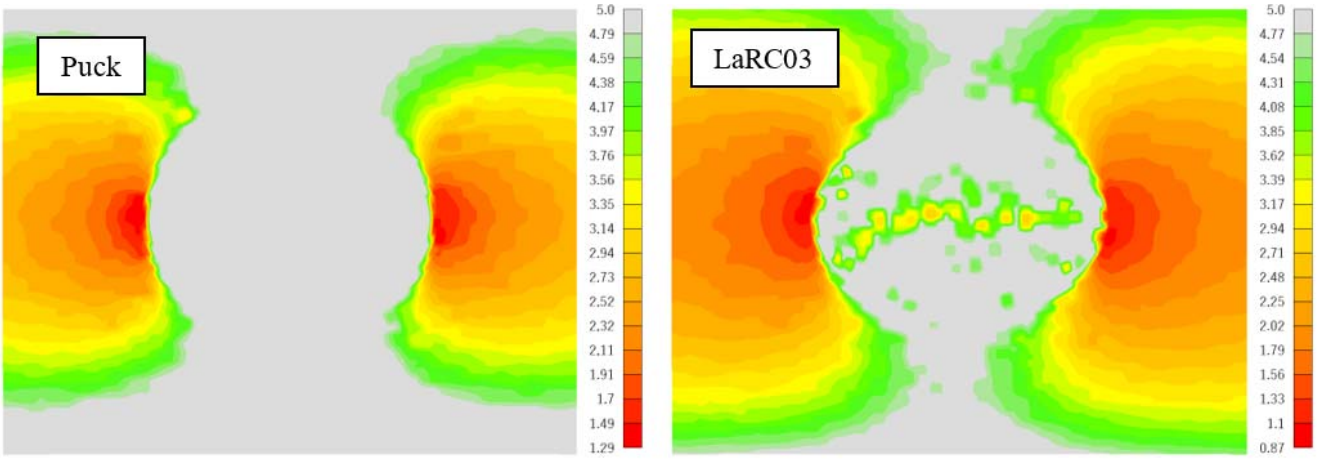

Figure 5. *Safetys factor at 0.59 ms for plate with defects*

Source: Puck and Schurmann (1998).

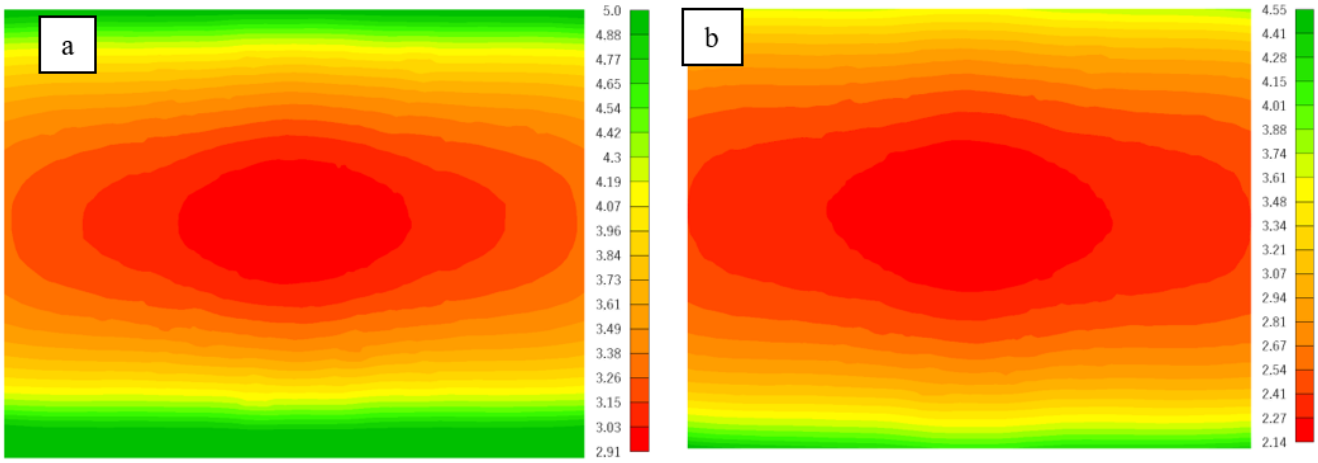

Figure 6. *Safety factor at 0.59 ms (without defects): a – a progressive damage model for laminated composites containing stress concentration, Failure criteria for unidirectional fiber composites, Failure analysis of FRP laminates by means of physically based phenomenological models; b – LaRC03*

Source: Hashin (1980), Chang and Chang (1987); Puck and Schurmann (1998).

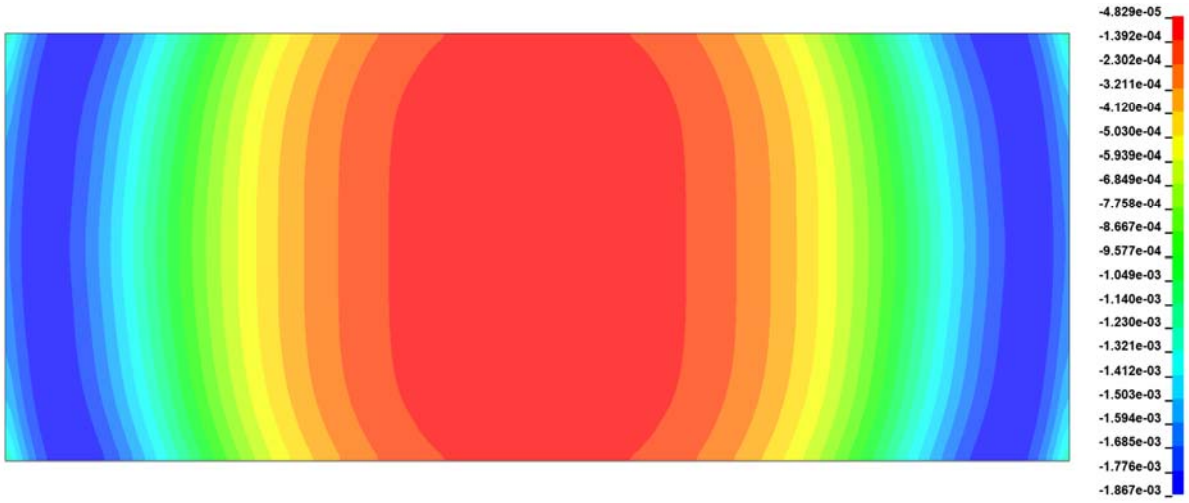

Figure 7. *Blast pressure on the plate at time 0.59 ms*

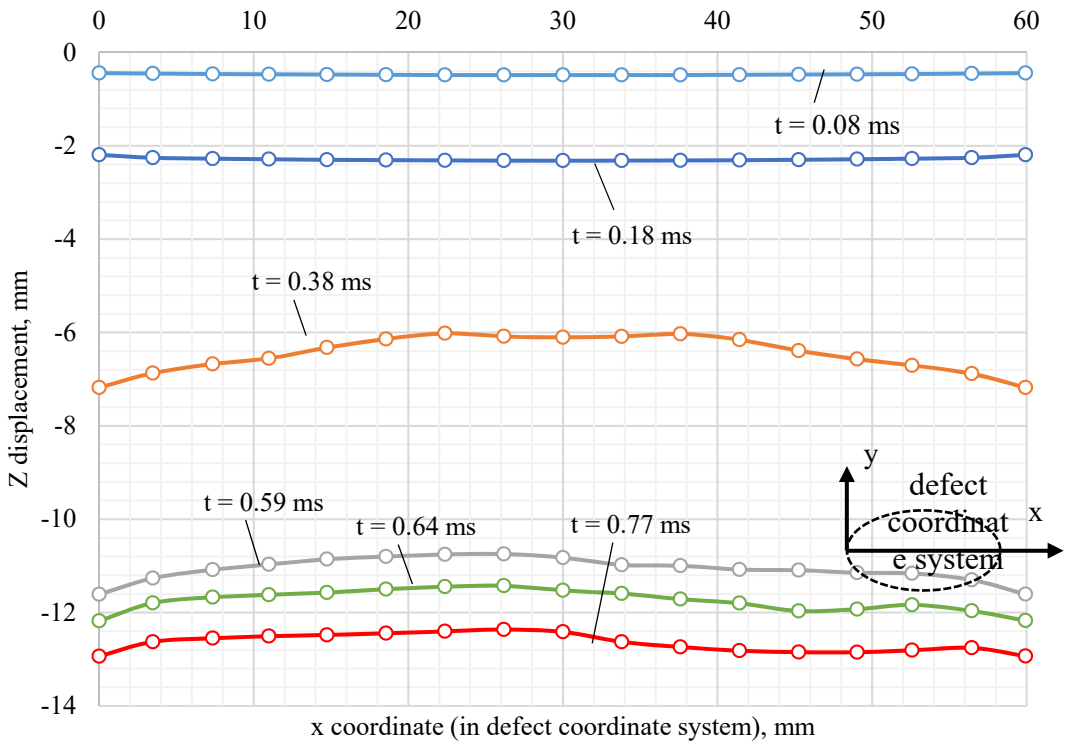

Figure 8. *Displacement of ply No. 10 in defect zone (plate with defects)*

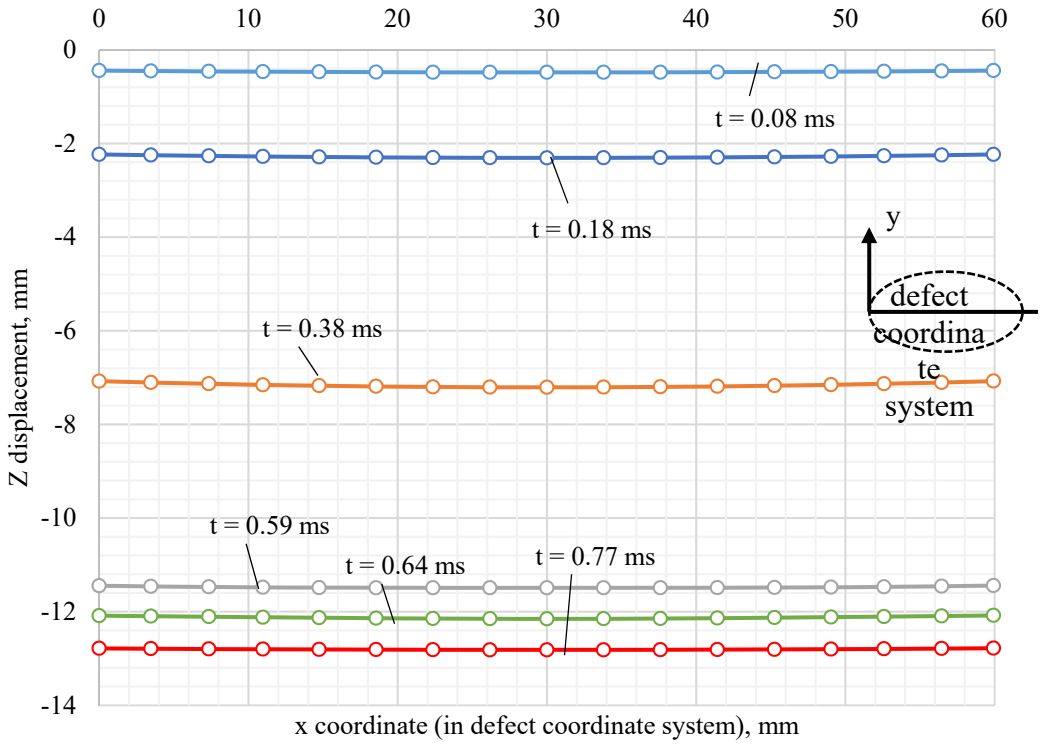

Figure 9. *Displacement of ply No. 10 in defect zone (plate without defects)*

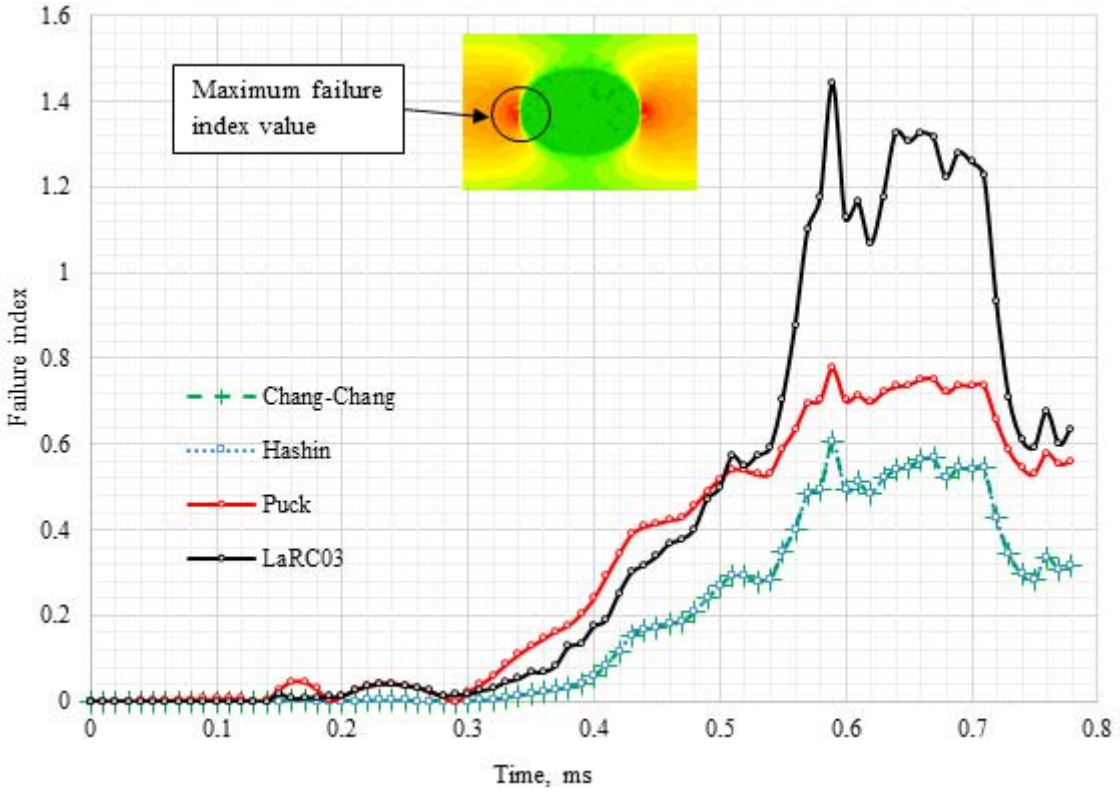

***Figure 10**. Failure index*